

# Modeling Of Beam Loss Induced Vacuum Breakdown in Heavy-Ion Rings

E.Mustafin<sup>1</sup>, I.Hofmann<sup>1</sup>, P.Spiller<sup>1</sup>,  
W.Fischer<sup>2</sup>, U.Iriso<sup>2</sup>, P.He<sup>2</sup>, H.C.Hseuh<sup>2</sup>, H. Huang<sup>2</sup>, V.Ptitsyn<sup>2</sup>, S.Y.Zhang<sup>2</sup>.

<sup>1</sup> *Gesellschaft für Schwerionenforschung mbH, Darmstadt, Germany,*

<sup>2</sup> *Brookhaven National Laboratory, Upton, USA.*

**Abstract.** The theory of dynamic vacuum pressure evolution in heavy-ion accelerators in presence of beam losses is discussed. Some particular cases are considered in more detail: average pressure evolution, steady-state vacuum pressure profile with account of beam losses, and pressure bumps induced by particle losses on the collimators. Practical applications to beam lifetime measurements at the SIS18 of GSI Darmstadt and desorption experiments at RHIC of BNL are considered.

## INTRODUCTION

Vacuum pressure rise induced by lost ions has been observed in several heavy-ion rings: in LEAR at CERN Geneva [1], in AGS Booster [2] and RHIC [3] at BNL Upton, and in SIS18 [4] at GSI Darmstadt. This has caused operational difficulties especially for low energy machines like LEAR, AGS Booster and SIS18. Test-stand measurements and machine experiments have been performed to measure desorption yields. In some cases modeling of the pressure evolution was necessary to determine the desorption yield from the measured pressure bumps. The method to describe the pressure evolution in heavy-ion machines in the presence of beam ion losses suggested in this paper allows to describe the average pressure rise in the machine as well as the self-consistent steady-state pressure profile in the approximation of persistent small beam particle losses.

## THE BASIC EQUATION

We will use a 1D diffusion type equation for the evolution of the linear pressure profile  $P(x,t)$  in the vacuum tube of the accelerator:

$$c(x)\frac{\partial^2 P}{\partial x^2} = -q(x) - q_h(x,t) + s(x)P + v(x)\frac{\partial P}{\partial t} \quad (1)$$

Here  $c$  is the specific linear conductance,  $q$  and  $q_h$  are the linear thermal and desorption outgassing,  $s$  is the linear pumping speed,  $v$  is the volume per unit length,  $x$  is the space and  $t$  the time coordinates. Initially, we consider equations for a single component residual gas only. Later in the paper we will consider more than one gas component whenever the single-gas approach fails to successfully describe the measurements.

One must supplement Eq.(1) with the appropriate initial conditions on the time coordinate and boundary conditions on the space coordinate. The latter is in general the periodicity condition of the vacuum system although different types of boundary conditions may be necessary for different measurement conditions (like a zero flow at closed valves, or an exponentially decreasing flow in long NEG-coated vacuum chambers with high linear pumping speed).

The desorption outgassing term  $q_h$  may be expressed as follows:

$$q_h = \frac{hsN}{T} \oint G(x,x')P(x')dx' \quad (2)$$

where  $h$  is the desorption coefficient,  $s$  is the beam particle loss cross-section,  $N$  is the number of beam ions,  $T$  is the beam revolution time. The function  $G(x,x')$  describes how many of beam particles lost at position  $x'$  in a slice  $dx'$  desorb at the vacuum chamber wall at position  $x$ . Because all lost particles will

eventually arrive at the vacuum chamber wall the  $G(x, x')$  is chosen to be normalized to unity:

$$\oint G(x, x') dx = 1 \quad (3)$$

## AVERAGE PRESSURE EVOLUTION

The beam life-time in the machine depends on the pressure averaged over the circumference  $L$ . The evolution of the average pressure  $\bar{P} = \oint P(x) dx / L$  can be derived from integration of Eq.(1):

$$-v \frac{d}{dt} \bar{P} + \left( \frac{hs}{T} N - s_{eff} \right) \bar{P} = -\bar{q} \quad (4)$$

Here the normalization Eq. (3) was taken into account. The effective linear pumping speed  $s_{eff} = \oint s(x) P(x) dx / \bar{P} L$  depends, in principle, on the pressure but within the accuracy of our model we neglected this dependency.  $\bar{q} = \oint q(x) dx / L$  is the average thermal outgassing. In the derivation of Eq.(4) we also neglected the weak dependence on the space coordinate of the linear volume and the specific conductance.

From Eq.(4) the pressure stability condition for small persistent beam losses reads:

$$\left( \frac{hs}{T} N - s_{eff} \right) < 0, \quad (5)$$

and the average pressure under the stable conditions is given as follows:

$$\bar{P} = \frac{\bar{P}_0}{1 - \frac{hsN}{Ts_{eff}}}, \quad (6)$$

where  $\bar{P}_0 = \bar{q} / s_{eff}$  is the static pressure in absence of beam losses.

In the case of considerable beam losses the intensity  $N$  cannot be taken to be time-independent and one must consider the beam life-time equation:

$$-\frac{d}{dt} N = \frac{SLn_L}{T} N \bar{P} \quad (7)$$

where  $n_L \approx 2.7 \cdot 10^{25} \text{ m}^{-3}$  is the number of molecules per cubic meter under the normal conditions. Simultaneous solution of Eq. (4) and Eq.(7) allows to find the parameters  $h$ ,  $s$ ,  $s_{eff}$  and  $\bar{P}_0$  from the beam life-time measurements. This procedure is applied in

[4] for the case of  $U^{28+}$  beam loss induced pressure rise in the SIS18.

## STEADY-STATE PRESSURE PROFILE

The pressure profile along the orbit in the presence of persistent beam losses may differ drastically from the static pressure without beam losses. The knowledge of the steady-state pressure profile under the beam loss induced desorption is important for determining the right distribution of the vacuum pump positions along the machine orbit.

The equation for the steady-state pressure profile may be obtained from Eqs.(1)-(2) by setting the time-derivative to zero:

$$c \frac{\partial^2 P}{\partial x^2} + \frac{hsN}{T} \oint G(x, x') P(x') dx' - s(x) P = -q(x). \quad (8)$$

It is interesting to note that with zero thermal outgassing the integro-differential equation Eq.(8) becomes a eigen-value problem for the parameter  $hsN/T$ , and corresponding eigen-functions  $P(x)$ . The lowest eigen-value  $hsN/T \approx s_{eff}$  corresponds to the stability threshold Eq.(5).

In Fig.1 the charge-exchange  $U^{28+} \rightarrow U^{29+}$  beam loss profile in the SIS18 is presented, corresponding to the solution of Eq.(8), i.e. the case when the lost particles experience the charge-exchange according to the local pressure. Also shown is the beam loss profile assuming a uniform distribution of charge-exchange events along the orbit.

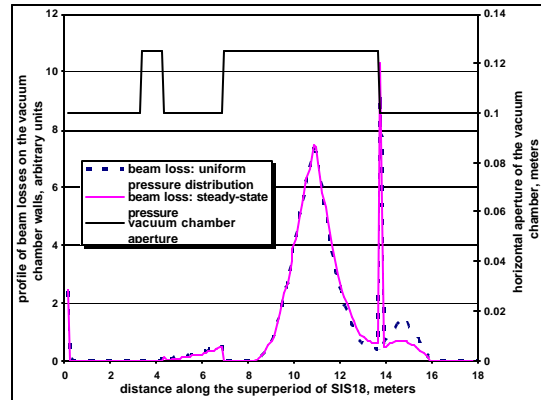


**FIGURE 1.** Profile of beam particle losses on the vacuum chamber wall of SIS18 superperiod: the red line is for the losses with corresponding charge-exchange rate proportional to the local pressure value, the dashed line is for the charge-exchange rate uniformly distributed along the circumference.

One notices a weak dependence of the pressure distribution on the loss profile. This is because the position of the beam ion losses is mostly determined by the bending magnets and the aperture limitations, and not by the locations where the ions experienced the charge-exchange.

## LUMPED PUMPING AND LOSSES ON COLLIMATORS

The equation for the steady-state pressure is extremely simplified in the case of lumped pumping and losses on collimators only:

$$c \frac{d^2}{dx^2} P = -q, \quad (9)$$

with boundary conditions at the collimator and pump positions:

$$c \frac{dP}{dx} \Big|_{x=x_k+0} - c \frac{dP}{dx} \Big|_{x=x_k-0} = k_k \frac{hsNL}{T} \bar{P} - S_k P_k \quad (10)$$

Here the coefficient  $k_k$  characterizes the fraction of the total beam loss that occurs at collimation position  $x_k$  ( $k_k=0$  if there is no collimator at this position) and  $S_k$  is the pumping speed at this position ( $S_k=0$  if there is no pump),  $P_k$  is the vacuum pressure value at  $x_k$ .

Suppose that all charge-exchange losses with U beam in the SIS18 are intercepted at the collimators equipped with local pumps. Then the pressure will not be affected by the lost beam desorption if the r.h.s. of Eq. (10) is zero, i.e.

$$S_k P_k \approx k_k \frac{hsNL}{T} \bar{P} \Rightarrow N \approx \frac{S_k T}{k_k hsL} \frac{P_k}{\bar{P}} \quad (11)$$

For a typical set of parameters  $h \approx 10^4$ ,  $s \approx 10^{-20}$  m<sup>2</sup>,  $P_k/\bar{P} \approx 1/2$ ,  $k_k \approx 1/48$  (we assume losses equally distributed onto four collimators in each of the 12 superperiods of SIS18),  $L \approx 217$  m (the orbit length),  $T \approx 4.5 \cdot 10^6$  s (for injection energy  $E \approx 11$  MeV/u),  $S \approx 2$  m<sup>3</sup>/s (of the order of ordinary titanium-sublimation pump) one finds  $N \approx 10^{10}$ .

As another example of our analysis method let us consider a desorption experiment with closed valves performed at RHIC, with the layout shown in Fig.2.

We consider a set of four measurements: #1: V1 closed, V2 open, blue beam; #2: V1 closed, V2 open, yellow beam; #3: V1 open, V2 closed, yellow beam; #4: V1 open, V2 closed, blue beam. The closed valves

were irradiated with continuous pulses of  $E_{kin} = 9$  GeV/u Au<sup>79+</sup> ions, and the pressure increase was measured with the ion gauge G3. Results of the analysis are shown in Table 1.

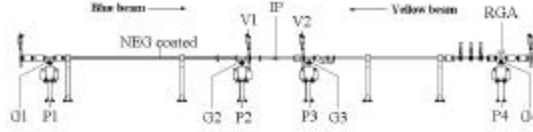


**FIGURE 2.** Layout of vacuum equipment: G denotes gauges, P pumps, V valves, RGA a residual gas analyzer, and IP the nominal beam interaction point. On the left hand side is a 5.15 m section with activated NEG coating.

**TABLE 1. RHIC desorption measurement data.**

Measurement	Ion rate, 1/s	DP, Torr	h
#1	$1.7 \cdot 10^8$	$1.9 \cdot 10^{-11}$	1100
#2	$1.4 \cdot 10^8$	$2.4 \cdot 10^{-11}$	1600
#3	$2.2 \cdot 10^8$	$0.6 \cdot 10^{-11}$	260
#4	$1.9 \cdot 10^8$	$0.6 \cdot 10^{-11}$	300

In this case the entire beam hit the valve (and a large part passed through) thus the first term in the r.h.s of Eq.(10) at the valve position should be:

$$0 - c \frac{dP}{dx} \Big|_{x=x_k-0} = h k T_{room} \dot{N} \quad (12)$$

where  $k=1.38 \cdot 10^{-23}$  J/K is the Boltzman constant,  $T_{room} = 293$  K the room temperature, and  $\dot{N}$  is number of ions per time that hit the closed valve (second column of Table 1). The term "0" in the l.h.s. of Eq. (12) means zero flow from the valve (besides the desorption described by the first term).

At the position of the gauge G3 the Eq. (10) has only a pumping term:

$$c \frac{dP}{dx} \Big|_{x=x_k+0} - 0 = -S_k \Delta P_k \quad (13)$$

where  $\Delta P_k$  is the observed pressure increase (third column of Table 1). The "0" term in the l.h.s. of Eq. (13) means zero flow towards the gauge G4 (there was no pressure rise observed at the G4 position).

Combination of Eq.(12) and Eq.(13) gives us a formula to calculate the desorption yield  $h$ :

$$h = \frac{S_k \Delta P_k}{\dot{N} k T} = \frac{S_k N_A}{\dot{N} V_{mole}} \frac{\Delta P_k}{P_{atm}}, \quad (14)$$

where  $S_k=270$  l/s is the pumping speed of the pump P3,  $N_A=6.02 \cdot 10^{23}$  is the Avogadro number,  $V_{mole}=22.4$  l is

the volume of the ideal gas under the normal conditions,  $P_{atm}=760$  Torr is the atmospheric pressure.

The resulting desorption yield values are shown in the last column of Table 1. A more detailed report of this measurement is in preparation [5].

## EQUATIONS WITH ACCOUNT OF THE SURFACE STAY TIME

In another RHIC desorption experiment the Au beam of energy  $E_{kin} = 9$  GeV/u was intentionally lost in a straight section and the pressure rise was measured in the three gauges pw3.1, pw3.2 and pw3.3.

An attempt to fit the pressure evolution observed in the gauges with the help of Eq.(1) was not successful: no reasonable set of parameters could explain the observed delay between the moment of beam impact and the time of the maximum pressure reading in the gauges, as it is shown in Fig.2.

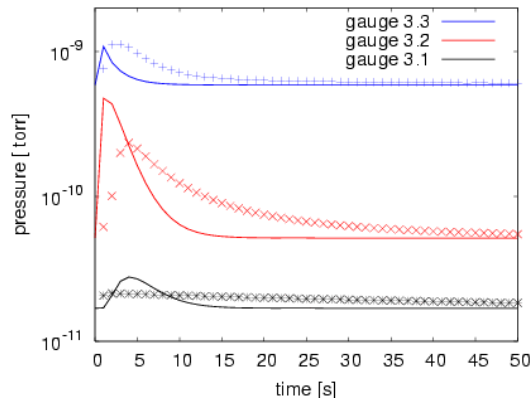


**FIGURE 2.** Measured pressure evolution and reproduced behavior using Eq.(1). Measurement and model differ for the readings in all three gauges.

We met two main difficulties with the fit to the measurement: a) Eq.(1) predicts a much shorter pressure bump arrival time compared to what was measured, b) the pressure rise and decay-times were longer in the experiment than it could be fit with Eq.(1). In order to explain the actual delay we a) considered a two component gas (the slow decay may be explained by the component with slow pumping time) and b) introduced one more term into Eq.(1), namely the term describing the surface stay time of the molecules:

$$v(x)\frac{\partial}{\partial t}P(t,x)-c(x)\frac{\partial^2}{\partial x^2}P(t,x)+s_1P(t,x)-s_2P(t-\mathbf{t},x)=q(x), \quad (15)$$

where the terms  $s_1P(t,x) - s_2P(t-\mathbf{t},x)$  describe sticking of molecules to the vacuum chamber wall at position  $x$  and time  $t$  with the linear pumping speed  $s_1$  and release of the molecules at the same position but with the time delay  $\mathbf{t}$  and linear desorbing speed  $s_2$ .

Eq.(15) describes the measured pressure evolution reasonably good as it is shown in Fig.3. More details on this experiment can be found in [6].

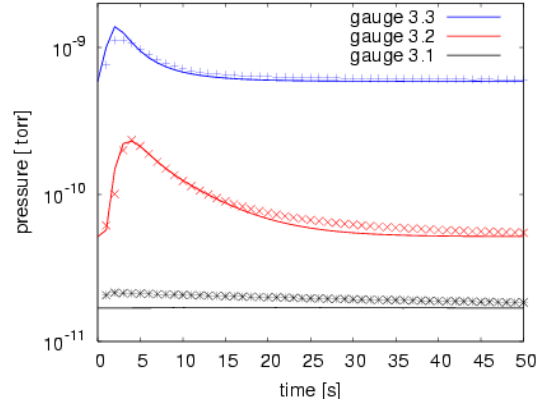


**FIGURE 3.** Measured pressure evolution (blue and red points) and reproduced behavior using Eq.(15) introducing surface stay time and a gas with two components.

## REFERENCES

1. S. Baird et al, "Recent Results on Lead-Ion Accumulation in LEAR for the LHC", CERN-PS/97-03 (DI), Geneva, Switzerland.
2. Zhang, S. Y., and Ahres, L. A., "Booster Gold Beam Injection Efficiency and Beam Loss" in *EPAC 98: Sixth European Particle Accelerator Conferenc*, edited by S Myers et al., AIP Conference Proceedings, New York: American Institute of Physics, 1998, pp. 2149-2151.
3. S.Y.Zhang, "RHIC Vacuum Pressure Bump", C-A/AP/67, January 2002.
4. E.Mustafin et al., *NIM A* **510**, 199-205 (2003).
5. W.Fischer et al., "Molecular desorption of stainless steel from irradiation with 9 GeV/u Au<sup>79+</sup> ions under perpendicular impact", in preparation.
6. U.Iriso et al, "Interpretation of desorption measurements of high-energy beams at RHIC", CAD/AP/178, November 2004.